

## Magnetoresistance in $\text{La}_{1-x}\text{Sr}_x\text{CoO}_3$ for $0.05 \leq x \leq 0.25$

Vladimir Golovanov and Laszlo Mihalý

*Department of Physics, State University of New York at Stony Brook, Stony Brook, New York 11794-3800*

A. R. Moodenbaugh

*Department of Applied Science, Brookhaven National Laboratory, Upton, New York 11973-5000*

(Received 3 November 1995)

The dc resistivity, magnetoresistance, and magnetic susceptibility of  $\text{La}_{1-x}\text{Sr}_x\text{CoO}_3$  compounds have been investigated in the temperature range of 4–300 K for magnetic fields up to 7 T. In the doping range studied ( $0.05 \leq x \leq 0.25$ ) the electronic properties of the material exhibit a crossover from semiconducting to metallic behavior. The magnetoresistance is highest in the semiconducting state. A correlation was found between the energy gap determined from the dc conductivity and the energy scale identified from neutron scattering data. The results are interpreted in terms of a double-exchange model.

The recent discovery of colossal magnetoresistance (MR) in thin films of La-Ca-Mn-O (Refs. 1,2) and giant magnetoresistance in a ferromagnetic perovskite of La-Ba-Mn-O (Ref. 3) generated a renewed interest in this family of compounds. Magnetization and resistivity studies of  $\text{La}_{1-x}\text{Sr}_x\text{MnO}_3$  single crystals<sup>4</sup> revealed several phases with the the highest magnetoresistance observed at the paramagnetic insulator to ferromagnetic metal transition. Neutron scattering measurements on  $\text{La}_{0.7}\text{Sr}_{0.3}\text{MnO}_3$  (Ref. 5) demonstrated that the ferromagnetism in  $\text{La}_{0.7}\text{Sr}_{0.3}\text{MnO}_3$  is itinerant in character.

Although most of the recent attention has been focused on the  $\text{MnO}_3$  perovskites, similar properties have been observed in materials based on  $\text{CoO}_3$ . The first studies of magnetic and transport properties of  $\text{La}_{1-x}\text{Sr}_x\text{CoO}_3$  by Jonker and van Santen<sup>6</sup> were interpreted by Goodenough.<sup>7</sup> Recently Señaris-Rodríguez and Goodenough performed extensive magnetic and transport studies of pure  $\text{LaCoO}_3$  (Ref. 8) and doped  $\text{La}_{1-x}\text{Sr}_x\text{CoO}_3$ .<sup>9</sup> Itoh *et al.*<sup>10</sup> deduced the magnetic phase diagram of  $\text{La}_{1-x}\text{Sr}_x\text{CoO}_3$  from magnetization measurements. Three phases were identified: at low temperatures spin-glass (for  $x < 0.18$ ) and cluster-glass (for  $x > 0.18$ ) phases and, at high temperatures, a paramagnetic phase. The magnetization dependence of the resistivity of  $\text{La}_{1-x}\text{Sr}_x\text{CoO}_3$  single crystals was investigated for  $x > 0.2$  by Yamaguchi *et al.*<sup>11</sup> The electronic structure of the material was studied near the semiconductor-metal transition in  $\text{La}_{1-x}\text{Sr}_x\text{CoO}_3$  by using electron spectroscopy.<sup>12</sup>

The negative magnetoresistance in the transition metal perovskites is usually interpreted in terms of the “double-exchange” mechanism, suggested by Zener,<sup>13</sup> and developed by Anderson<sup>14</sup> and de Gennes.<sup>15</sup> The principal idea is that most of the electrons on the outer shells of the transition metal reside on localized orbits, coupled by Hund’s rule to large magnetic moments, whereas others participate in the conduction *via* overlapping orbits. Due to the exchange interaction between the two types of electrons, the conduction is conditional on the appropriate orientation of the underlying localized moments. A related approach, suggested for metals by de Gennes and Friedel<sup>16</sup> and adapted to semiconductors by Haas *et al.*,<sup>17</sup> treats the magnetic moments in a

mean field approximation. The “perfect” ferromagnetic order leads to a spin splitting of the conduction band, whereas the magnetic disorder is viewed as a source for extra scattering processes.

The magnetoresistance, and the electrical conduction in general, is strongly influenced by the spin state of the Co ions, which was the subject of recent neutron scattering measurements by Asai *et al.*<sup>18</sup> Motivated by this study, we investigated the low- and high-field magnetization, dc electrical resistivity, and the magnetoresistance, for magnetic fields up to 7 T, on a set of ceramic samples of composition  $\text{La}_{1-x}\text{Sr}_x\text{CoO}_3$ . In contrast to the work by Yamaguchi *et al.*,<sup>11</sup> we concentrated on the low doping range  $0.05 \leq x \leq 0.25$ .

$\text{La}_{1-x}\text{Sr}_x\text{CoO}_3$  polycrystalline samples were prepared by the solid state reaction method similar to that described in Ref. 10. The appropriate mixture of  $\text{La}_2\text{O}_3$ ,  $\text{SrCO}_3$ , and  $\text{CoO}$  was ground and calcined repeatedly at 950 °C for 10 days, fired at 1300 °C for about 28 h and then cooled in air at a rate of approximately 100 °C/h. This cooling rate is considered to be “fast,” as opposed to “slow” cooling rate of 100 °C/day used by Itoh *et al.*<sup>10</sup> Fast cooling (60 °C/h) has been also used in the recent work of Señaris-Rodríguez and Goodenough.<sup>9</sup> The samples were confirmed to be of a single phase with rhombohedrally distorted perovskite structure by powder x-ray diffraction analysis. The low-field magnetic properties of the samples produced here agreed well with the published results<sup>10</sup> and the resistivity curves for  $x=0.2$  and 0.25 were similar to those obtained in Ref. 9. We found, however, that the temperature-dependent resistivities of different cuts from the same specimen were different. In order to remedy this shortcoming, we performed an additional heat treatment at 950 °C for 5 h and we cooled the samples slowly, at a rate of 100 °C per day as suggested by Itoh *et al.*<sup>10</sup> After the heat treatment the low-field magnetic properties did not change significantly, but the resistivity did: In contrast to the fast-cooled specimens<sup>9</sup> the resistivity curves for  $x=0.2$  and 0.25 had a positive slope for the whole temperature range measured. The resistivity measurements were very reproducible for all compositions. The data reported here were obtained on the slow-cooled material.

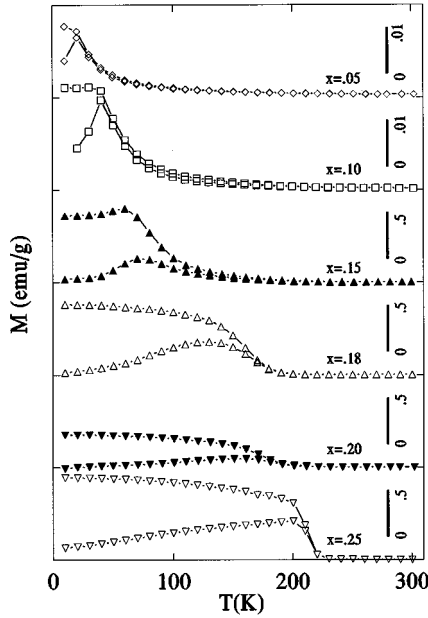


FIG. 1. Low-field magnetization measurements on samples of various Sr content  $x$ . For each  $x$ , the lower magnetization was obtained in the zero-field-cooled measurement, the higher one corresponds to field cooling. The curves are shifted for better view; the high-temperature magnetization is close to zero for each samples. The vertical bars indicate the magnetization scale. For  $x=0.05$  and  $x=0.1$  the scale is expanded by a factor of 50.

Magnetization measurements were performed using a superconducting quantum interference device (SQUID) magnetometer in low (20 G) and high (50 kG = 5 T) magnetic fields. For the low-field measurements the samples were first cooled in zero magnetic field (ZFC measurement), then in the 20-G magnetic field (FC measurement). A difference between the ZFC and FC data indicates a magnetic phase with permanent magnetization and hysteresis in the magnetization curve. To estimate the saturation magnetization of the system we took ZFC data for the high field.

The electrical resistance was measured as a function of temperature and magnetic field in a superconducting magnet with the maximum applied field of  $H=7$  T. The samples were rectangular in shape and about  $10 \times 5 \times 2$  mm in size. Four electrical leads were glued with silver paste, in line, along the long axis of the specimen. The outside leads were used to supply the current. The voltage drop was measured on the inside leads. The direction of current was perpendicular to magnetic field. The linearity in the current-voltage dependence has been checked at several temperatures and magnetic fields; for the range of currents used here the resistivity proved to be Ohmic for all samples.

To investigate the magnetoresistance we swept the magnetic field at several fixed temperatures. This method gives a

high accuracy (especially for semiconductor samples, where a temperature lag between the sample and the thermometer could easily lead to a resistance difference larger than the magnetoresistance), and it also provides a full picture of the possible nonlinearity and hysteresis of the MR.

Magnetization measurements on our samples (Fig. 1) led to results similar to those observed by Itoh *et al.*<sup>10</sup> At the higher  $x$  values the samples exhibit ferromagnetism, with a Curie temperature of 220 K for  $x=0.25$ . At low  $x$  the magnetic response is much weaker; note the difference in the scale for the upper two curves in Fig. 1. This behavior was interpreted by Itoh *et al.*<sup>10</sup> as evidence for a spin-glass-like phase.

The high-field magnetizations at 10 K are presented in Table I along with the average magnetizations per Co and per Sr atoms in units of  $\mu_B$ . We found about 30% higher magnetization than Señaris-Rodríguez and Goodenough<sup>9</sup> did for similar compositions. The high-field magnetization per Co atom measured by Itoh *et al.*<sup>10</sup> on the  $x=0.5$  sample is also higher than that reported in Ref. 9. The difference may be due to the different cooling rates of the samples.

According to the data, the magnetization per Co atom increases approximately linearly with doping concentration. Each Sr atom brings five to seven spins to the system. The high value of magnetization per Sr site indicates that each dopant atom converts about two Co atoms into a high- (or intermediate-) spin configuration.

In Fig. 2 the solid lines represent the dc resistivity of the samples. The room temperature resistivity of the  $x=0.2$  sample turned out to be higher than that of the  $x=0.18$  compound. A systematic error, caused by geometrical factors, may be responsible for this.<sup>19</sup> In the figure the curve corresponding to  $x=0.18$  was scaled up and the curve corresponding to  $x=0.20$  was scaled down by a factor of 1.4. For low concentrations of Sr the samples are semiconductors. There are two distinct energy gaps in the semiconducting state: at higher temperatures ( $>30$  K) the conductivity is characterized by a larger gap; at low temperatures ( $<30$  K) a lower gap is observed. The crossover behavior is common for doped semiconductors;<sup>20</sup> we will discuss this matter later. For  $x=0.18$  the conductivity shows the signs of a metal-insulator transition. The resistivity of this sample drops dramatically at high temperature and approaches the metallic resistance of the highly doped samples. The magnitude and temperature dependence of the resistivity of the  $x=0.20$  and 0.25 samples is metallic.

In the Mn analog of the material, the highest magnetoresistance has been observed in the neighborhood of the ferromagnetic transition. Figure 3 illustrates that a similar behavior was found in our metallic samples: There is a MR peak near the Curie temperature of the  $x=0.18-0.25$  compounds. However, we found even larger values of MR in the semiconducting phase, and the highest MR was observed in the

TABLE I. Magnetizations of  $\text{La}_{1-x}\text{Sr}_x\text{CoO}_3$  for different  $x$  at 5 T and 10 K.

$x$	0.05	0.10	0.15	0.18	0.20	0.25
Magnetization (emu/g)	8.24	11.62	19.14	29.05	31.88	36.31
Magnetic moment per Co atom ( $\mu_B$ )	0.36	0.50	0.82	1.23	1.34	1.52
Magnetic moment per Sr atom ( $\mu_B$ )	7.2	5.0	5.4	6.8	6.7	6.1

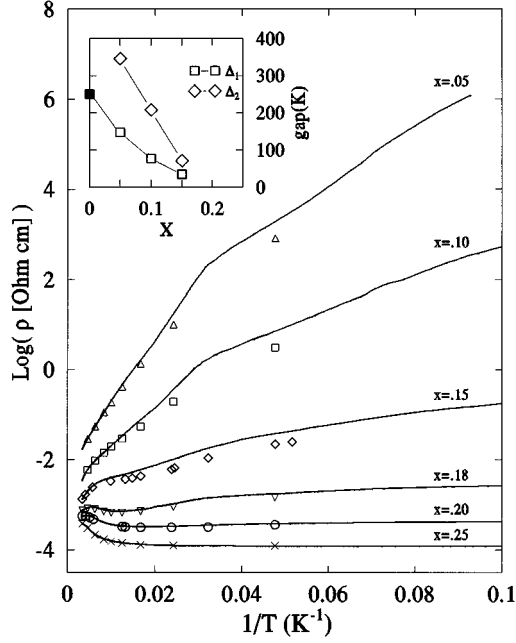


FIG. 2. Logarithm of resistivity vs. inverse temperature for a set of samples of various doping level  $x$ . The solid line is the result of the measurement in zero magnetic field. Note the crossover between two distinct activation energies for low  $x$  and the metallic behavior at high  $x$ . The symbols are resistivities measured in  $H=7$  T. The inset shows (open symbols) the activation energies evaluated from the slopes of resistivity curves for semiconducting samples. Also shown in the inset (solid square) is the energy gap obtained for the  $x=0$  sample from thermal expansion measurements by Asai *et al.* (Ref. 18). The solid line in the inset is guide to the eye.

low-temperature spin-glass regime. The magnetoresistance exhibits a hysteresis as it follows the internal magnetic fields in the sample, which lags behind the externally applied magnetic field (Fig. 3, inset). The resistivity in the 7-T magnetic field, as obtained from field sweeps similar to that shown in the inset of the Fig. 3, is represented in Fig. 2 by open symbols.

In order to understand the electronic transport in the doped samples, we first consider the pure material  $\text{LaCoO}_3$ . The ground state electronic configuration of Co atom is  $t_{2g}^6 e_g^0$  with zero spin.<sup>8</sup> The thermal excitation of Co atoms to the high-spin  $t_{2g}^4 e_g^2$  ( $\text{Co}^{3+}$ ) state is responsible for the anomalous thermal expansion of pure  $\text{LaCoO}_3$ .<sup>18</sup> The concentration  $n$  of excited Co atoms can be estimated as<sup>18</sup>

$$n = \frac{\nu}{\nu + \exp(\Delta/k_B T)}, \quad (1)$$

where  $\nu=15$  is the multiplicity of the high-spin state. Remarkably, the Co low-spin  $\rightarrow$  high-spin transition gap in pure  $\text{LaCoO}_3$ , estimated from thermal expansion,<sup>18</sup> coincides very well with the activation energy determined from our low-temperature resistivity measurements, if the data are extrapolated to  $x=0$  (Fig. 2, inset). This coincidence suggests that the low-temperature conduction is intimately related to the thermal activation of high-spin states with a gap modified with doping, presumably due to lattice distortion. At high temperatures another activated process dominates

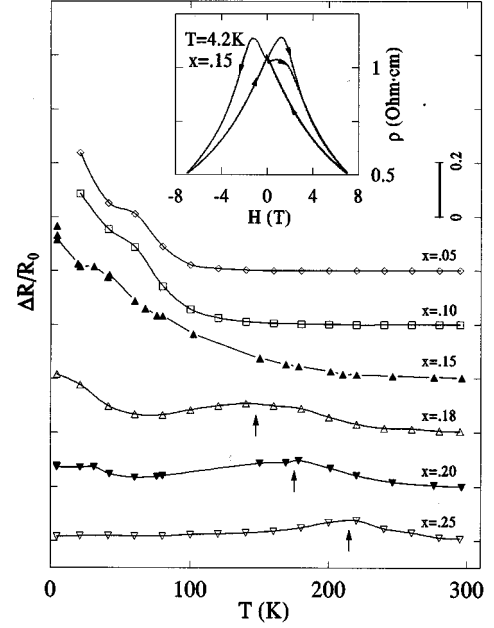


FIG. 3. Magnetoresistance  $\Delta R/R_0$  as a function of temperature. The curves are shifted along the vertical axis for better view and the MR scale is indicated by the bar on the upper left side. The MR is close to zero at room temperature for all samples. The arrows indicate the ferromagnetic transition temperature.

the conduction, characterized by a conductivity of  $\sigma_2 \exp(-\Delta_2/k_B T)$ . The experimental data for  $x=0.05, 0.10,$  and  $0.15$  in Fig. 2 are reasonably well fitted by the empirical formula

$$\rho^{-1} = \sigma_1 n' + \sigma_2 \exp(-\Delta_2/k_B T), \quad (2)$$

where  $n' = \nu / [\nu + \exp(\Delta_1/k_B T)]$  is the number of excited  $\text{Co}^{3+}$  atoms. The parameters  $\sigma_1, \Delta_1, \sigma_2, \Delta_2$  are  $0.025 \Omega^{-1} \text{cm}^{-1}, 140 \text{K}, 150 \Omega^{-1} \text{cm}^{-1}, 340 \text{K}$  for  $x=0.05$ ;  $0.66 \Omega^{-1} \text{cm}^{-1}, 90 \text{K}, 400 \Omega^{-1} \text{cm}^{-1}, 210 \text{K}$  for  $x=0.10$ ;  $0.20 \Omega^{-1} \text{cm}^{-1}, 40 \text{K}, 500 \Omega^{-1} \text{cm}^{-1}, 80 \text{K}$  for  $x=0.15$ , respectively.

In  $\text{La}_{1-x}\text{Sr}_x\text{CoO}_3$  the dopant Sr introduces high-spin ( $t_{2g}^3 e_g^2$ )  $\text{Co}^{4+}$  into the system.<sup>12</sup> An electron residing on the thermally excited  $\text{Co}^{3+}$  can move to the  $\text{Co}^{4+}$  sites via double exchange. At low temperature, when  $n' \ll x$ , the charge transport happens by hopping between  $\text{Co}^{4+}$  sites where the number of carriers is determined by the number of excited  $\text{Co}^{3+}$  atoms. The overlap between the corresponding orbitals depends strongly on the doping level. This explains the small value and strong (exponential)  $x$  dependence of the factor  $\sigma_1$  in Eq. (2).

At temperatures above 30 K the number of excited  $\text{Co}^{3+}$  becomes greater than the dopant concentration  $x$ ; therefore it is more appropriate to consider an array of  $\text{Co}^{3+}$  sites to which  $\text{Co}^{4+}$  donates a hole that can jump, again using double exchange. The resulting band is nearly full, and the number of holes is  $x$ , resulting in a  $\sigma_2$  which scales approximately linearly with the doping. Disorder causes localization of the electronic states close to the band edge in the vicinity of the Fermi level. Nevertheless, since nearly all Co sites participate in the conduction, the overlap

integral is large, leading to high mobility carriers at an energy  $\Delta_2$  below the Fermi energy. This is in accordance with  $\sigma_2 \gg \sigma_1$ .

The highest magnetoresistance was observed at low doping levels and low temperatures, where Itoh *et al.*<sup>10</sup> suggested spin-glass behavior. The double-exchange conduction in this state is strongly affected by the disorder in the spin distribution. This disorder is partially suppressed by external magnetic field resulting in high, negative magnetoresistance.

In our metallic samples the MR is 5 times smaller than that observed in the spin-glass state, and it is also much smaller than the MR of the  $\text{MnO}_3$  perovskites. In a recent work, Millis *et al.*<sup>21</sup> argue that double exchange cannot be the sole source of the anomalous large magnetoresistance in the  $\text{LaSrMnO}$  compound. They suggest that the Jahn-Teller

effect due to the displacement of oxygen around the  $\text{Mn}^{3+}$  ion plays an important role. This mechanism sensitively depends on the presence of an unpaired electron on the upper  $e_g$  level and therefore may not be active in our samples. In accordance with the arguments of Millis *et al.*, the significantly lower value of MR in Co compounds corresponds to the double-exchange mechanism alone.

The authors wish to thank J. M. Tranquada for initiating this study and for useful discussions, and L. Henderson Lewis for help in sample preparation. Work at SUNY, Stony Brook, is supported by the NSF Grant No. DMR9321575. Work at BNL is supported by the U.S. Department of Energy, Division of Materials Science, under Contract No. DE-AC02-76CH00016.

- 
- <sup>1</sup>S. Jin *et al.*, *Science* **264**, 413 (1994).  
<sup>2</sup>M. McCormack, S. Jin, T.H. Tiefel, R.M. Fleming, J.M. Phillips, and R. Ramesh, *Appl. Phys. Lett.* **64**, 3045 (1994).  
<sup>3</sup>R. von Helmholtz, J. Wecker, B. Holzapfel, L. Schultz, and K. Samwer, *Phys. Rev. Lett.* **71**, 2331 (1993).  
<sup>4</sup>A. Urushibara, Y. Moritomo, T. Arima, A. Asamitsu, G. Kido, and Y. Tokura, *Phys. Rev. B* **51**, 14 103 (1995).  
<sup>5</sup>M. Martin, G. Shirane, Y. Endoh, K. Hirota, Y. Moritomo, and Y. Tokura (unpublished).  
<sup>6</sup>G.H. Jonker and J.H. van Santen, *Physica* **19**, 120 (1953).  
<sup>7</sup>J.B. Goodenough, *J. Phys. Chem. Solids* **6**, 287 (1958).  
<sup>8</sup>M.A. Señarís-Rodríguez and J.B. Goodenough, *J. Solid State Chem.* **116**, 224 (1995).  
<sup>9</sup>M.A. Señarís-Rodríguez and J.B. Goodenough, *J. Solid State Chem.* **118**, 323 (1995).  
<sup>10</sup>M. Itoh, I. Natori, S. Kubota, and K. Motoya, *J. Phys. Soc. Jpn.* **63**, 1486 (1994).  
<sup>11</sup>S. Yamaguchi, H. Taniguchi, H. Takagi, T. Arima, and Y. Tokura, *J. Phys. Soc. Jpn.* **64**, 1885 (1995).  
<sup>12</sup>A. Chainani, M. Mathew, and D.D. Sarma, *Phys. Rev. B* **46**, 9976 (1992).  
<sup>13</sup>C. Zener, *Phys. Rev.* **82**, 403 (1951).  
<sup>14</sup>P.W. Anderson and H. Hasegawa, *Phys. Rev.* **100**, 675 (1955).  
<sup>15</sup>P.-G. de Gennes *Phys. Rev. B* **118**, 141 (1959).  
<sup>16</sup>P.-G. de Gennes and J. Friedel, *J. Phys. Chem. Solids* **4**, 71 (1958).  
<sup>17</sup>C. Haas, A.M.J.G. van Run, P.F. Bongers, and W. Albers, *Solid State Commun.* **5**, 657 (1967).  
<sup>18</sup>K. Asai, O. Yokokura, N. Nishimori, H. Chou, J.M. Tranquada, G. Shirane, S. Higuchi, Y. Okajima, and K. Kohn, *Phys. Rev. B* **50**, 3025 (1995).  
<sup>19</sup>Similar effects has been experienced for  $x=0.2$  and  $x=0.3$  by P. Ganguly, P.S.A. Kumar, P.N. Santhosh, and I.S. Mulla, *J. Phys. Condens. Matter* **6**, 533 (1994).  
<sup>20</sup>N. Ashcroft and N. Mermin, *Solid State Physics* (Saunders College, Philadelphia, 1976), p. 565.  
<sup>21</sup>A.J. Millis, P.B. Littlewood, and B.I. Shraiman, *Phys. Rev. Lett.*, **74**, 5144 (1995).